J. Fluid Mech. (1993), *vol.* 248, *pp.* 153–172

The interaction of deep-water gravity waves and an annular current: linear theory

By MARIUS GERBER

Department of Applied Mathematics, Stellenbosch University, Stellenbosch, South Africa

(Received 21 March 1990 and in revised form 2 October 1992)

The interaction of linear, steady, axisymmetric deep-water gravity waves with pre-existing large-scale annular currents has been investigated. Waves originating inside the annulus as well as waves approaching the annulus from the outside were studied. Exact linear ray solutions were obtained and involve two non-dimensional parameters, a radius-angle parameter and a velocity parameter. For opposing currents the linear solutions also allow the derivation of radii at which the waves are blocked, reflected at a linear caustic or stopped by the current. Various examples of rays interacting with an annular current are presented to illustrate aspects of the solutions obtained. In particular, the behaviour of the ray solutions at blocking, reflection and stopping is investigated. Linear ray theory is shown to fail at caustics and caustic solutions are briefly discussed.

1. Introduction

The interaction of surface gravity waves and water with a non-uniform current distribution is important in a number of different contexts. Waves near the coastline and beaches may be significantly influenced by tidal currents and wind-driven currents. On a larger scale, the strong western-boundary currents of oceans can, and do, strongly affect ocean waves. Recent relevant papers are by Gerber (1991), who discussed the generation of giant waves in the Agulhas Current, and Holthuijsen & Tolman (1991), who used a third-generation numerical wave model to study effects of the Gulf Stream on ocean waves in swell and storm conditions.

Much of the significant theoretical work in this field makes use of a short-wavelength or 'refraction' approximation to describe the variation of the waves. That is, the lengthscale of the current distributions is assumed to be much greater than the wavelength of the waves and an approximation equivalent to the geometric optics approach for light propagation can be justified. This so-called plane-wave ansatz leads to hyperbolic-type initial value problems. The first-order approximation then gives an 'eikonal' equation for the wave rays and the second-order approximation a transport (wave-action) equation for the wave amplitude. Meyer (1979) gives a more complete review.

The emphasis of this paper is on the linear theory of the interaction of deep-water waves, generated on still water, and pre-existing large-scale currents. Longuet-Higgins & Stewart (1960, 1961) were the first to give an accurate description of linear wave–current interactions and introduced the concept of radiation stress. Further contributions to our understanding of the interaction of linear waves and large-scale currents came from, among others, Whitham (1962), Bretherton & Garrett (1968) and Peregrine (1976), who examined a number of different situations.

In almost all of the above studies the analysis was confined to two special

situations of steady currents, namely (i) straight currents, varying with distance along the stream or (ii) straight currents varying across the stream. Exact linear solutions for these situations were derived by Longuet-Higgins & Stewart (1960, 1961). Here we extend the range of known linear solutions by considering the simplest formulation of interaction with a curved current, namely steady axisymmetrical waves on an axisymmetrical annular current. This restriction simplifies the mathematics but, even so, solutions have been found for a wide range of cases.

In this study, as in all the work mentioned above, we consider an ideal flow and disregard the fact that regions of shear in the current are always turbulent. Any really effective treatment should also include the time-varying properties of the flow. However, Savitsky (1970) found that even small mean currents can be more important than the effects of smaller-scale turbulence so the simplification to steady flow may be a good approximation.

In many circumstances the waves may be refracted, leading to considerable non-uniformities of wave energy. The ray calculations then frequently lead to crossed rays, which correspond to singularities of the ray approximation. For small-amplitude waves the plane-wave approximation can usually be improved where rays meet at a caustic. The maximum steepness of the caustic solution will then indicate whether the small-amplitude approximation remains valid or not. Uniformly valid small-amplitude approximations which include reflection-type caustics have been developed by McKee (1974) and Peregrine & Smith (1975, 1979), while Peregrine (1976) gives details for waves at a stopping velocity caustic.

A noteworthy situation involving caustics occurs off the south-east coast of South Africa. The interaction of large south-westerly swells with the opposing Agulhas Current produce sporadic giant waves and have caused extensive damage to shipping (Mallory 1974). Ships wishing to take advantage of the strong Agulhas Current, which flows down the coast at 4–5 knots, have encountered waves with very steep leading edges and with wave height of the order of 20 m. Smith (1976) studied the generation of giant waves on the Agulhas Current. He assumed the current to be steady and irrotational and investigated wave reflections at a straight caustic. He derived a relevant nonlinear Schrödinger equation which described the behaviour of the wave amplitude. An asymmetric wave profile and wave peaks with steep leading edges were found, which is in agreement with what is known of the prototype. The validity of Smith's assumption of a straight caustic must, however, be questioned. The stretch of Agulhas Current under consideration (north of approximately 34° S) is not straight, but closely follows the curvature of the south-east coast of South Africa. Neither can existing analytical ray solutions adequately model the 'upstream' reflections of waves initially outside an opposing straight shear current.

The purpose of this paper is to extend the linear theory of the interactions of waves with a large-scale current to more general current situations. The study was motivated by the inability of the linear theory of parallel shear flows to reflect incident waves, initially outside the current, and opposing the flow direction. The present linear theory indicate that when the waves and current propagate in the same direction, but with some angle of incidence between the current and the wave rays, the waves will be refracted by the current until the rays become parallel to the current. At this point the waves will not penetrate the current any further but will be reflected back out. When the waves approach a straight opposing shear current at some angle, a different situation is described. In this case the wave rays will be refracted towards the propagation direction of the current and may even be swept

downstream by the current. Reflection, as described above, will not take place and the rays will eventually penetrate the current. However, for waves initially outside the current, numerical modelling has indicated that 'upstream reflections' (that is reflection of the waves on an opposing current) can take place on curved currents. It is anticipated that this reflection may lead to very steep waves which cannot be described by infinitesimal-wave theory.

The mathematical description of steady linear axisymmetrical waves on an axisymmetrical annular current is present in §2. Exact linear solutions for convex and concave currents are presented. In §3 the particular solutions, corresponding to waves being reflected, blocked and stopped by the current, are discussed. Various examples are also presented in §4 to elucidate the difference between these features. Energy considerations are discussed in §3. In §6 the validity of the plane-wave and small-amplitude approximations is discussed while the relevant linear caustic solution is briefly discussed in §7. Conclusions are presented in §8.

2. Mathematical formulation

The kinematics of a train of surface gravity waves in the presence of a slowly varying current $\boldsymbol{U}(\boldsymbol{x})$ are characterized by a wavenumber $\boldsymbol{k}(\boldsymbol{x}, t)$ and an intrinsic frequency $\sigma(\boldsymbol{k})$ (two-dimensional horizontal vectors are assumed unless otherwise indicated). The dispersion relation gives the functional dependence of σ on $\boldsymbol{k}$ and for linear deep-water waves:

$$\sigma^2 = gk, \quad k = |\boldsymbol{k}|.$$

The apparent frequency, i.e. the frequency of waves passing a fixed point, is

$$\omega = \sigma(\boldsymbol{k}) + \boldsymbol{k} \cdot \boldsymbol{U}. \tag{2.1}$$

Consistency relations between ω and $\boldsymbol{k}$ are given by (i) the kinematical conservation equation for the density of waves,

$$\partial \boldsymbol{k}/\partial t = -\boldsymbol{\nabla}\omega, \tag{2.2}$$

and (ii) the condition that the distribution of the local wavenumber vector in space is irrotational:

$$\boldsymbol{\nabla} \times \boldsymbol{k} = 0. \tag{2.3}$$

Consider now, in polar coordinates, an annular current of the form

$$\boldsymbol{U} = U_\theta(r)\, \boldsymbol{e}_\theta, \tag{2.4}$$

where r and θ are the polar coordinates and $\boldsymbol{e}_\theta$ is a unit vector in the θ-direction. Equation (2.4) describes an axisymmetric current with arbitrary velocity profile which is a function of the radial distance only.

For a steady axisymmetric wave field, with wavenumber $\boldsymbol{k} = k_r \boldsymbol{e}_r + k_\theta \boldsymbol{e}_\theta$, (2.3) becomes

$$(\mathrm{d}/\mathrm{d}r)\,(rk_\theta) = 0. \tag{2.5}$$

Locally, for α, the angle between the wavenumber $\boldsymbol{k}$ and the unit vector $\boldsymbol{e}_r$ in the radial direction, (2.5) then gives (see figure 1)

$$rk_\theta = rk \sin\alpha = rk \sin(\phi - \theta) = m, \tag{2.6}$$

where ϕ is the angle between $\boldsymbol{k}$ and the x-axis and m is a constant.

The apparent frequency (2.1) now becomes

$$\omega = \sigma + kU_\theta \sin\alpha = k[c + U_\theta \sin\alpha], \tag{2.7}$$

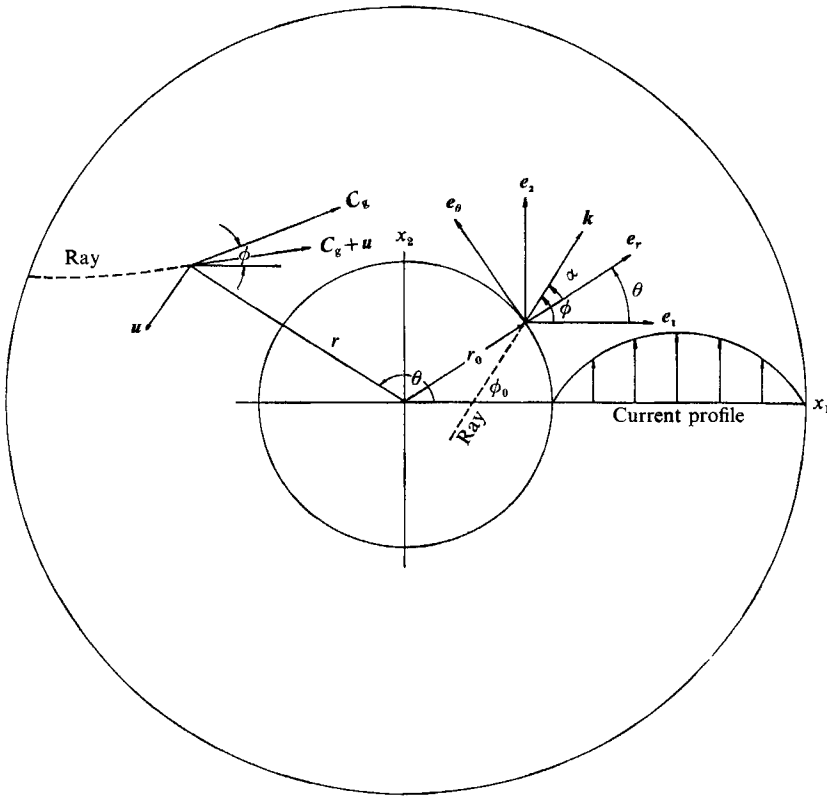

FIGURE 1. Definition diagram of rays interacting with an annular current.

where $c = \sigma/k$, since $\boldsymbol{U}$ does not have a component in the U_r-direction. On substitution of (2.6), and by using the linear dispersion relation, (2.7) becomes

$$\omega = k[c+mU_\theta/rk] = g/c+mU_\theta/r.$$

Thus
$$c = \frac{g}{\omega - mU_\theta/r} \quad \text{and} \quad k = \frac{(\omega - mU_\theta/r)^2}{g}. \tag{2.8}$$

Finally, from (2.6)

$$\sin\alpha = \frac{m}{rk} = \frac{mg}{r(\omega - mU_\theta/r)^2} \tag{2.9}$$

on substitution from (2.8).

For a wave ray initially outside the influence of the current (where the wavenumber $k = k_0$ and the phase speed $c = c_0$), (2.7), (2.8) and (2.9) become

$$c_0 = \frac{g}{\omega}, \quad k_0 = \frac{\omega^2}{g}, \quad \sin\alpha_0 = \frac{mg}{r\omega^2}.$$

Then
$$\frac{c}{c_0} = \frac{1}{1 - mU_\theta/r\omega}, \tag{2.10}$$

$$\frac{k}{k_0} = (1 - mU_\theta/r\omega)^2, \tag{2.11}$$

$$\frac{\sin\alpha}{\sin\alpha_0} = \frac{1}{(1 - mU_\theta/r\omega)^2}. \tag{2.12}$$

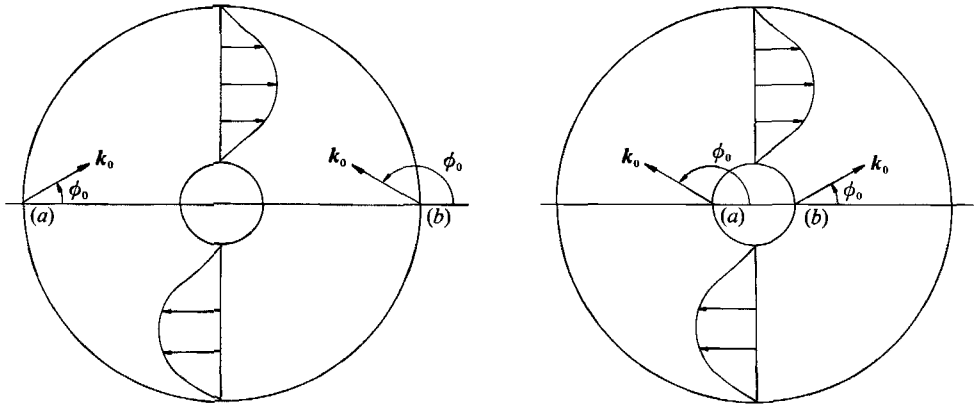

Convex currents
(*a*) $R = 1$; $\phi_0 < 90°$
(*b*) $R = 1$; $\phi_0 > 90°$
Inside annulus: $R < 1$.

Concave currents
(*a*) $R = 1$; $\phi_0 > 90°$
(*b*) $R = 1$; $\phi_0 < 90°$
Inside annulus: $R > 1$.

FIGURE 2. Definition diagram for concave and convex currents.

In order to interpret the above relations, it is convenient to specify the outside (or inside) radius of the annulus at the point of entry of the ray. Let the radius of the current at this point be r_0. Assume further that $U_\theta = 0$ just outside (inside) the annulus, i.e. where $r \to r_0$. From the symmetry of the current it is clear that, without loss of generality, a polar angle $\theta_0 = 0$ can then be selected for the point of entry r_0. Since $\alpha = \phi - \theta$, $\alpha_0 = (\phi - \theta)_0$ and the angle between $\boldsymbol{k}$ and the x-axis at r_0 is then ϕ_0 (see figure 1). Equations (2.10), (2.11) and (2.12) then become

$$c = \frac{c_0}{1-(r_0/r)\,(U_\theta/c_0)\sin\phi_0}, \tag{2.13}$$

$$k = k_0[1-(r_0/r)\,(U_\theta/c_0)\sin\phi_0]^2, \tag{2.14}$$

$$\sin\alpha = \frac{(r_0/r)\sin\phi_0}{[1-(r_0/r)\,(U_\theta/c_0)\sin\phi_0]^2}. \tag{2.15}$$

By introducing the dimensionless variables $C = c/c_0, K = k/k_0$, $R = r/r_0$ and $V = U_\theta/c_0$, equations (2.13), (2.14) and (2.15) can be written as

$$C = \frac{R\,\mathrm{cosec}\,\phi_0}{R\,\mathrm{cosec}\,\phi_0 - V}, \tag{2.16}$$

$$K = \left[\frac{R\,\mathrm{cosec}\,\phi_0 - V}{R\,\mathrm{cosec}\,\phi_0}\right]^2, \tag{2.17}$$

$$\sin\alpha = \frac{R\,\mathrm{cosec}\,\phi_0}{[R\,\mathrm{cosec}\,\phi_0 - V]^2}. \tag{2.18}$$

We now introduce the terminology that for rays initially outside the annulus, which then penetrate the circular current at $R = 1$, so that $R < 1$ within the annulus where $V \neq 0$, the term *convex current* (to the direction of wave approach) will be used. Conversely, *concave currents* have waves that originate inside the annulus before they penetrate the annulus at $R = 1$. R will then become greater than unity within the annulus where $V \neq 0$. Figure 2 is a schematic representation of convex and concave currents as defined above.

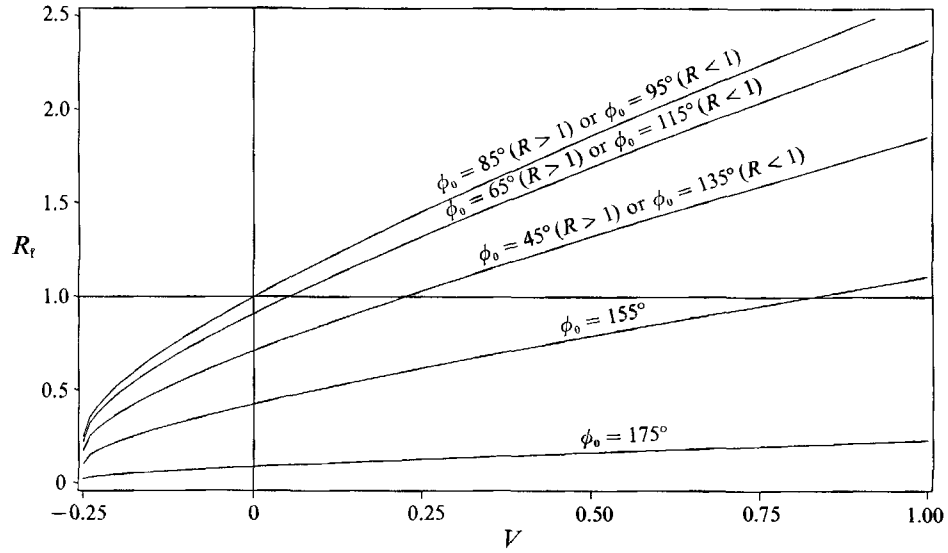

FIGURE 3. The radius at reflection, R_f, as a function of V for various initial angles ϕ_0. Note that an initial angle ϕ_0 for $R > 1$ (concave currents) corresponds to $180° - \phi_0$ for $R < 1$ (convex currents).

3. Special solutions

It is clear that the right-hand side of (2.18) can have a magnitude greater than one for the range of V-values. This defines upper and lower limits to V for which solutions exist. The critical velocities bounding the region without waves are

$$V = R \operatorname{cosec} \phi_0 \pm (R \operatorname{cosec} \phi_0)^{\frac{1}{2}}. \tag{3.1}$$

At these critical velocities $\alpha = 90°$ so that the waves travel parallel to the current. In practice the rays are tangent to a caustic curve, concentric with the eddy, and reflection of the rays result. It is important to note that with this model the wave motion along rays is entirely reversible. Note also that 'reflection' in this paper implies $\alpha = 90°$ and $V \neq 0$. The corresponding circular caustic curve is thus at a fixed radius from the origin within the current. For axisymmetrical wave fields caustics can, however, also occur in the absence of 'reflection'. This is when the wave rays cross within the core of the annulus and although $\alpha = 90°$, $V = 0$.

Equation (2.18) allows us to solve for the linear radius at reflection, $R_f = (r/r_0)_f$, as a function of V,

$$R_f = \tfrac{1}{2} \sin \phi_0 [1 + 2V \pm (1 + 4V)^{\frac{1}{2}}], \tag{3.2}$$

where the positive root of (3.2) is consistent with the usual choice of negative root for (3.1). The reflection radius, R_f, is shown graphically in figure 3 for a range of incident angles ϕ_0. It is clear from figure 3 that, unlike for straight shear currents, reflection of the wave field is now also possible for waves initially outside an opposing current, but since reflection for $V < 0$ is only possible for $R < 1$, only for currents convex to the direction of wave approach.

For currents opposing the direction of wave approach two other refraction configurations, at other α angles, may also be identified. 'Blocking' is when the component of the group velocity in the direction of $\boldsymbol{e}_\theta$, $C_g \sin \alpha$, becomes equal to $|U_\theta|$:

$$C_g \sin \alpha + U_\theta = 0, \tag{3.3}$$

and the waves are blocked in the $\boldsymbol{e}_\theta$-direction. This is shown schematically in figure

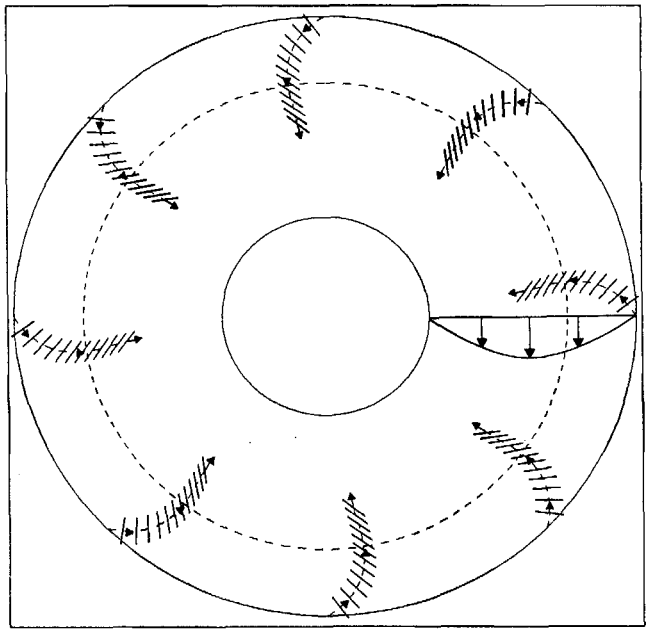

FIGURE 4. Schematic representation of axisymmetrical waves blocked by an opposing convex annular current. Eight individual wave rays with corresponding wave crests are shown. The radius at which each ray is blocked by the current is shown by the dashed line.

4. As in the case of reflection a fixed 'blocking radius' from the origin may also be identified. Note also that at the blocking position all the wave rays have a radial orientation.

The second, or 'stopping', configuration results when the local group velocity of the waves becomes equal and opposite to the convection velocity of the current:

$$C_g + U_\theta \sin\alpha = 0. \tag{3.4}$$

The crests of the waves are refracted to be parallel to the ray direction and the waves are stopped in the k-direction. Figure 5 is a schematic representation of waves stopped by the current. As before, a fixed 'stopping radius' from the origin may be identified.

The blocking condition, equation (3.3), can be investigated further. On substitution of (2.13), with $C_g = \frac{1}{2}c$, and (2.15) into (3.3) the following expression for the blocking radius R_b, where $R_b = (r/r_0)_{\text{block}}$, is obtained:

$$2VR_b \operatorname{cosec}\phi^0[1 - V/(R_b \operatorname{cosec}\phi_0)]^3 + 1 = 0. \tag{3.5}$$

The radius at blocking, corresponding to different adverse current values V, can then be calculated from (3.5) for different incident angles ϕ_0. For the blocking radius shown in figure 4, $\phi_0 = 120°$ and $V = -0.28$.

The stopping velocity condition (3.4) can also be investigated further (see Phillips 1978): Consider a steady wavetrain. Equation (2.7), for a constant frequency ω, gives

$$k[c + U_\theta \sin\alpha] = k_0 c_0,$$

where k_0 and c_0 are the constant wavenumber and phase-velocity parameters in still water. Since

$$c = (g/k)^{\frac{1}{2}}, \quad c_0 = (g/k_0)^{\frac{1}{2}},$$

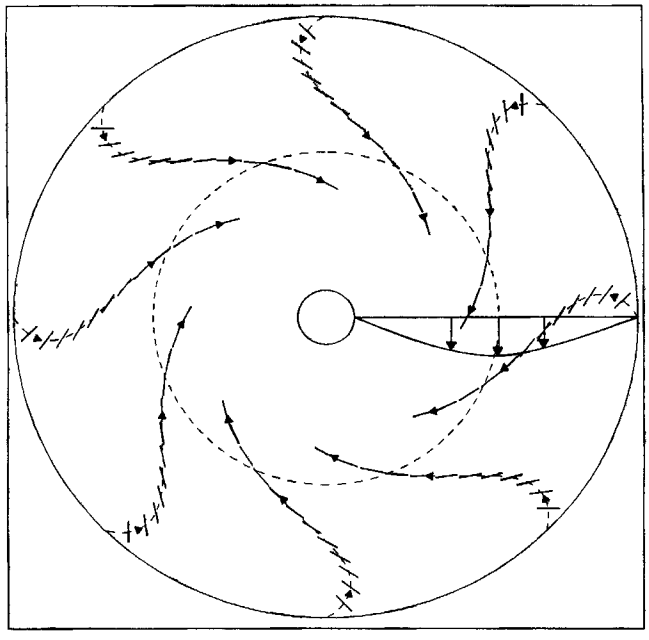

FIGURE 5. As figure 4 for but axisymmetrical waves stopped by an opposing convex annular current.

a quadratic equation in $C = c/c_0$ results:

$$C^2 = K^{-1} = C + V \sin \alpha.$$

The solution is

$$C = \frac{1}{2} + \frac{1}{2}[1 + 4V \sin \alpha]^{\frac{1}{2}},$$

which implies that

$$V \sin \alpha \geqslant -\tfrac{1}{4}. \tag{3.6}$$

At the caustic the equality will apply. Equation (3.6) defines the limit to the adverse current velocity, for different (V, α) combinations, at which the waves will be stopped. The waves will therefore be stopped in the k-direction for a range of α-values, as shown by (3.6), and only at reflection when $V = -\frac{1}{4}$ and α becomes equal to 90° will the reflection and stopping conditions occur simultaneously.

The linear radius at stopping, $R_s = (r/r_0)_{\text{stop}}$, can also be obtained from (3.6). Substitution of (2.18) into (3.6), with equality being applied, gives

$$R_s = -V/\text{cosec}\, \phi_0, \tag{3.7}$$

which is independent of α. For the stopping radius shown in figure 5, $\phi_0 = 120°$ and $V = -0.5$.

By using (2.16) and (2.17) the dimensionless celerity C and dimensionless wavenumber K may be contoured in the $(R \text{ cosec } \phi_0, V)$-plane. Superposition of the current profile, as a function of the radius R and the initial angle ϕ_0, $V(R \text{ cosec } \phi_0)$, then provides an easy mechanism to study the variation of the waves. Both C and K contours are straight lines through the origin of the $(R \text{ cosec } \phi_0, V)$-plane. Similarly, if the resultant α-values of (2.18) are contoured in the $(R \text{ cosec } \phi_0, V)$-plane

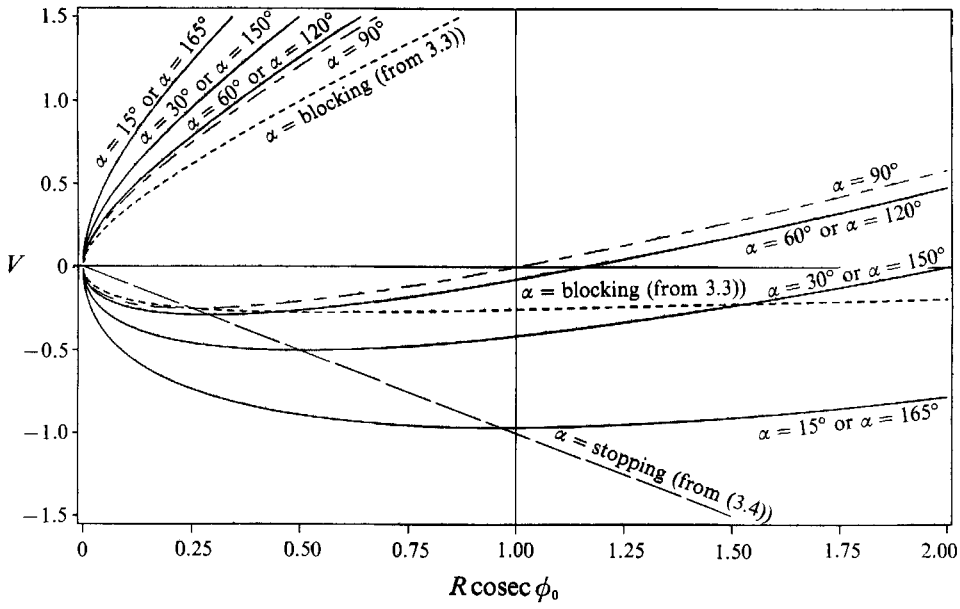

FIGURE 6. Contours of α on the (R cosec ϕ_0, V)-plane. The $\alpha = 90°$ contour is also the reflection contour. The blocking and stopping contours are also shown.

the contours of figure 6 are obtained. The intersection of the various contours with the R cosec ϕ_0-axis then indicate the cosec ϕ_0-values of the initial ϕ_0 entry angles, that is where $R = 1$ and $V = 0$. Since for concave (convex) currents $R > 1$ ($R < 1$), the abscissa values in figure 6 will be increasing (decreasing) from the initial cosec ϕ_0-value when rays penetrate the annulus from the concave (convex) side.

The $\alpha = 90°$ contour in figure 6 is of particular interest since it represents the linear caustic curve where reflection of the wave rays take place. Other important contours in figure 6 are those which indicate where the rays are blocked or stopped by the current. These contours were obtained from (3.3) and (3.4). It is clear that only the lower branch of the blocking contour in figure 6 is relevant. Figure 6 also shows that for waves initially on still water, for both concave and convex currents, the blocking condition will always occur before the stopping condition can be satisfied. Furthermore, in practical applications the linear stopping velocity condition will only be satisfied for waves of relatively short period. This is due to the relatively large opposing current values needed for (3.4) to apply.

4. Numerical ray solutions

Waves interacting with a shearing current can, in general, exhibit four different types of behaviour. That is, the waves can (i) penetrate the current, (ii) be reflected by the current, (iii) become blocked by the current or (iv) be stopped by the current. Whereas all four of these types of behaviour can be expected from waves opposed to the flow direction of the current, waves that propagate in the same direction as the current cannot be blocked or stopped by the current.

The information contained in figure 6 is very useful since it allows us to illuminate the different features of straight, concave and convex shearing currents. For example, for given initial angle of incidence, ϕ_0, different annular current

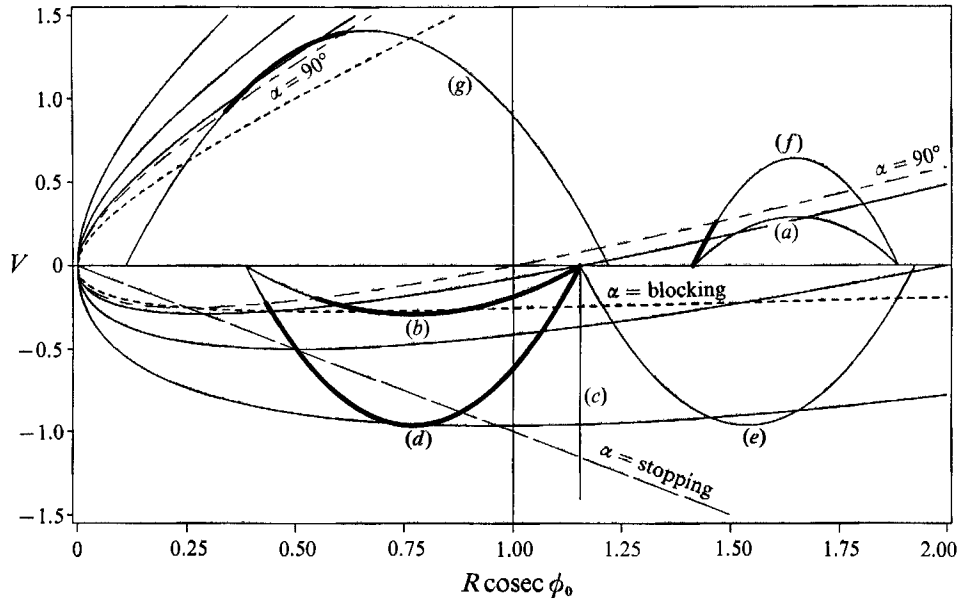

FIGURE 7. The annular current configuration used to generate the wave ray examples of figures 8–14. In cases of reflection of the waves, only the bold parts of the current profiles are relevant.

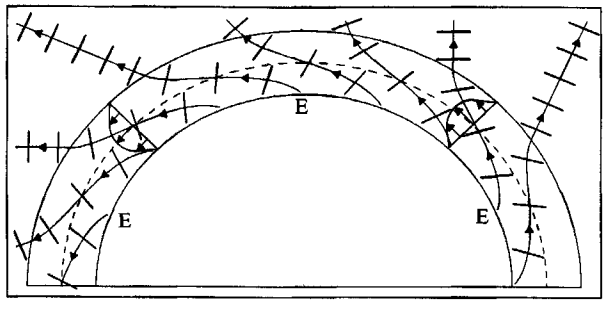

FIGURE 8. Example 1: a family of wave rays penetrating the following concave annular current marked (*a*) in figure 7. The initial angle between the ray and the x-axis $\phi_0 = 45°$ so that R cosec $\phi_0 = 1.41$. The value of the current parameter $V_{max} = 0.28$. The points of entry of the rays are marked E.

distributions of the form (2.4) may be superimposed on the (R cosec ϕ_0, V)-plane and the variation of the waves followed graphically. Various numerical ray simulations of an axisymmetrical wave field interacting with an annular current of the form (2.4) are shown in figures 8–14. The point of entry of the rays in each of these figures is marked by E while the maximum current velocity within the annulus is indicated by a dashed line. The wave crests are also shown in some of these figures. For each of these figures the corresponding parabolic current profile is shown in figure 7. In particular instances where the waves are reflected by the current the relevant part of the current profile is indicated by a bold line. Also, the position on the ray where the waves are blocked, reflected and stopped by the current are shown by the filled circles marked B, F and S in figures 8–14.

Figure 8 shows a family of rays penetrating the following concave annular current marked (*a*) in figure 7. The initial angle between the ray and the x-axis, ϕ_0, was taken

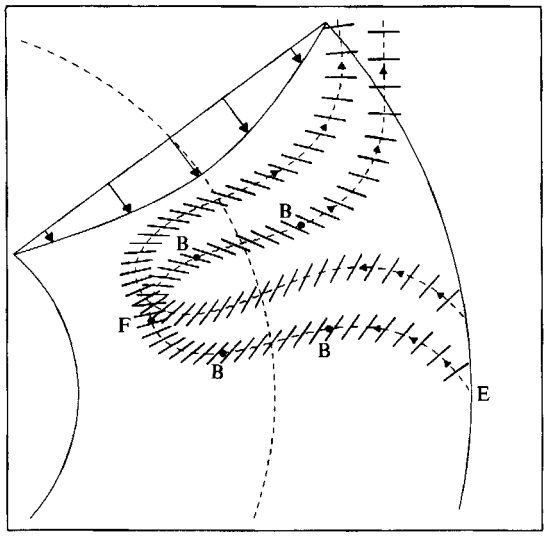

FIGURE 9. Example 2: two wave rays blocked and reflected by the opposing convex annular current marked (*b*) in figure 7. $\phi_0 = 120°$ so that R cosec $\phi_0 = 1.15$; and $V_{max} = 0.28$. The points of entry, blocking and reflection of the rays are marked E, B, and F, respectively.

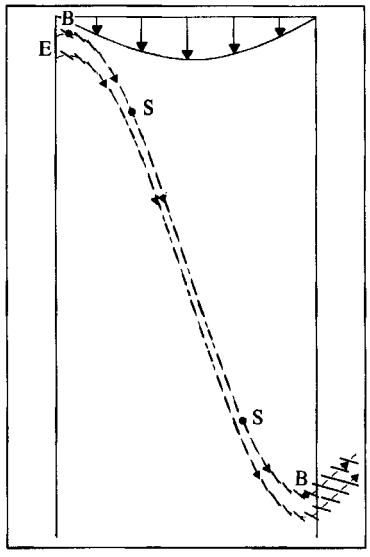

FIGURE 10. Example 3: two wave rays blocked and stopped by the opposing straight current marked (*c*) in figure 7. $\phi_0 = 60°$ so that R cosec $\phi_0 = 1.15$; and $V_{max} = -0.96$. The points of entry, blocking and stopping of the rays are marked by E, B and S, respectively.

as 45°, corresponding to R cosec $\phi_0 = 1.41$. The maximum value of the parameter V occurs at the dashed centreline radius of the annulus and for this example $V_{max} = 0.28$.

Figure 9 is an example of two rays interacting with the opposing convex current marked (*b*) in figure 7. The initial angle $\phi_0 = 120°$ so that R cosec $\phi_0 = 1.15$. Only the bold part of the profile is relevant since the waves are reflected by the current. The filled circles in figure 9 correspond to the positions where the waves are blocked before being reflected by the current. Since the wave motion along the rays is

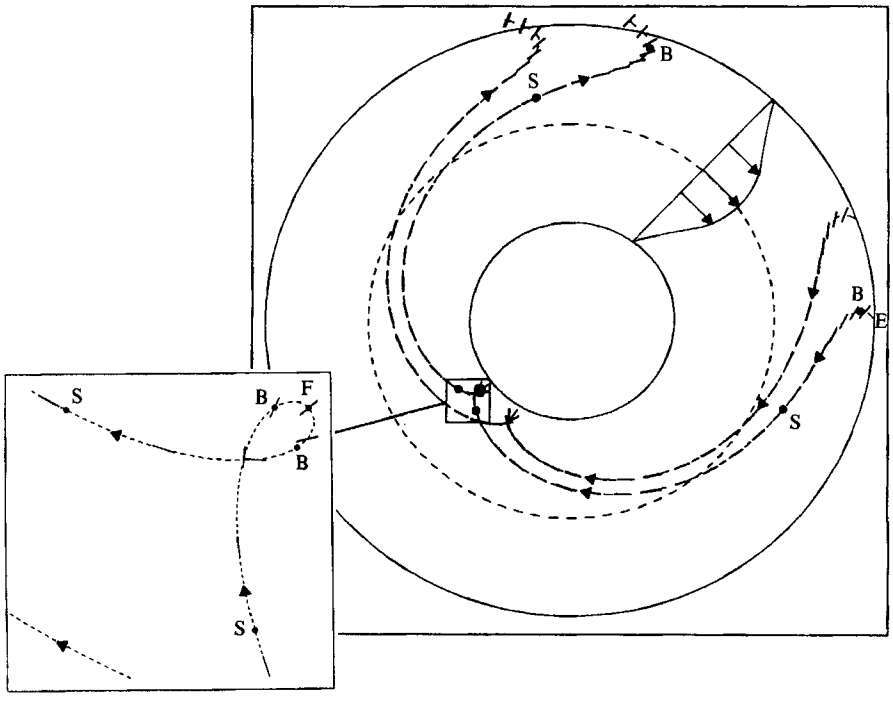

FIGURE 11. Example 4: two wave rays blocked, stopped and reflected by the opposing convex annular current marked (*d*) in figure 7. $\phi_0 = 120°$ so that R cosec $\phi_0 = 1.15$; and $V_{max} = -0.96$. The points of entry, blocking, stopping and reflection of the rays are marked by E, B, S and F, respectively.

reversible, the blocking contour is crossed twice (figure 7) before the waves exit the annulus.

It is interesting to note that on a straight opposing current, such as the current marked (*c*) in figure 7, reflection of the waves is not possible. This is also shown in figure 10. As before, the filled circles indicate the positions where the waves are blocked and stopped by the current. The waves are only stopped at relatively large values of V; in this example $V_{max} = -0.96$.

Figure 11 is another example of waves interacting with an opposing convex current. Here the dimensionless current velocity, V, is such that the waves are both blocked and stopped before they reflect. The initial angle of incidence is, similar to that of figure 9, taken as $\phi_0 = 120°$ and the relevant current profile is marked (*d*) in figure 7. The value of $V_{max} = -0.96$. The current profile marked (*e*) in figure 7 was used to generate the rays in figure 12. This profile is similar to that used in figure 11, except that here the waves approach the opposing current from the concave side.

Waves may also be trapped by an annular current. Waves generated on still water, before interacting with a concave current, may undergo multiple reflections within a certain radius and thus become trapped inside the annulus. Figure 13 is a trapped ray solution corresponding to the current profile marked (*f*) in figure 7. The angle of initial incidence $\phi_0 = 45°$ while $V_{max} = 0.64$.

For this annular configuration, and for waves initially inside the annulus while propagating in the same direction as the current, it can also be seen from figure 7 that profiles that reach up to the upper branch of the caustic line $\alpha = 90°$ may have trapped waves on them for chosen initial conditions. Figure 14 is an example of such

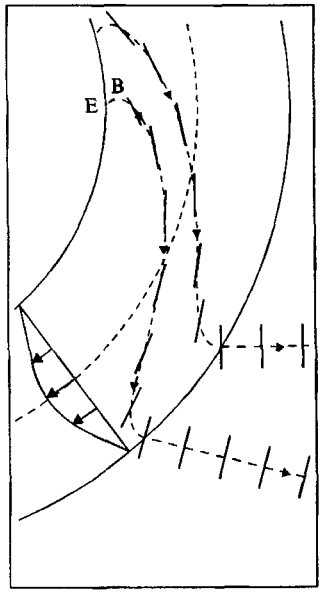

FIGURE 12. Example 5: two wave rays blocked before penetrating the opposing concave annular current marked (*e*) in figure 7. $\theta_0 = 60°$ so that R cosec $\phi_0 = 1.15$; and $V_{max} = -0.96$.

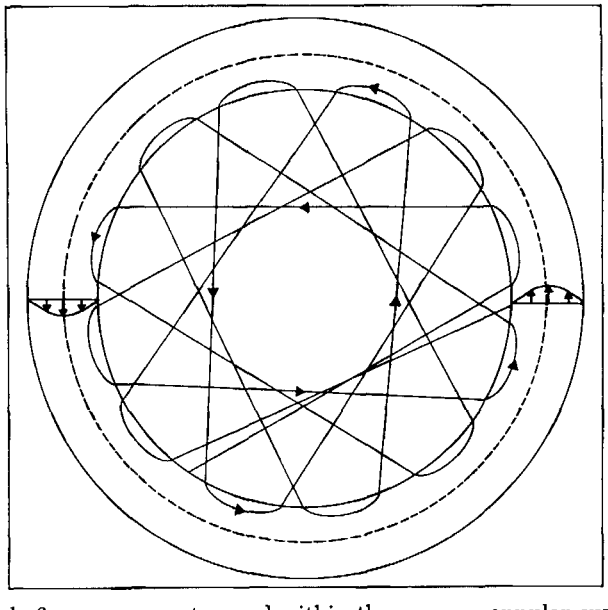

FIGURE 13. Example 6: a wave ray trapped within the concave annular current marked (*f*) in figure 7. $\phi_0 = 45°$ so that R cosec $\phi_0 = 1.41$; and $V_{max} = 0.64$.

a single trapped ray. The bold part of the current profile marked (*g*) in figure 7 corresponds to the ray solution shown in figure 14. It is clear that relatively large V-values are needed to trap the waves. In this example $V_{max} = 1.4$.

The parabolic nature of the contact of the caustic contour $\alpha = 90°$ with the V-axis in figure 7 also shows that (for $K \neq 0$) the wave rays can only reach $R = 0$, i.e. become radially oriented so that there is a focus of rays at the origin, when $\phi_0 = 0$ (and $m = 0$). Otherwise (2.17) shows that, as $R \to 0$, $K \to \infty$, giving the so-called short-

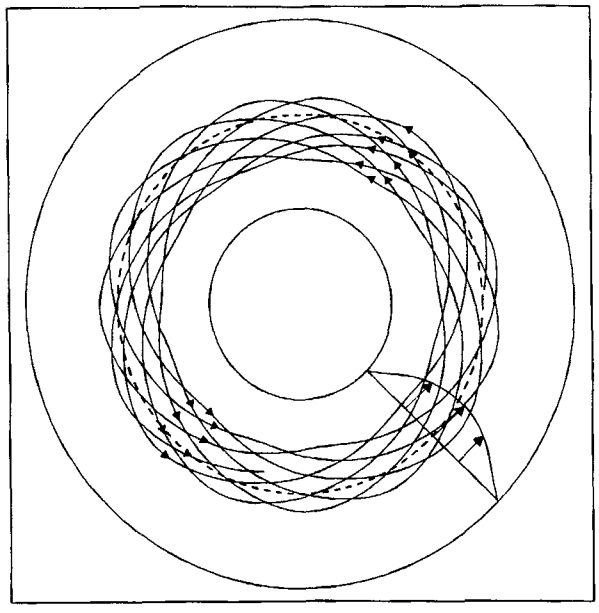

FIGURE 14. Example 7: a wave ray trapped within the following annular current marked (g) in figure 7.

wavelength singularity. This is when waves are refracted so much that the wavelength becomes very short and the small-amplitude approximation is no longer valid since the waves become too steep. The case $\omega = 0$ also corresponds to $R \to 0$ (for $K \neq 0$) as can be seen on substitution for c and $\sin\alpha$ in (2.7).

5. Energy considerations

The specification of the wave field is completed by use of the wave-action conservation equation (Peregrine & Smith 1979):

$$(\partial/\partial t)(G_\omega a^2) - \nabla\cdot(G_k a^2) = 0. \tag{5.1}$$

Here

$$G(\omega, \boldsymbol{k}, \boldsymbol{x}) = 0 \tag{5.2}$$

is the linear dispersion relation for an inhomogeneous medium, $G_\omega a^2 \equiv A = E/\sigma$ is the wave-action density and $G_k a^2 \equiv \boldsymbol{B} = (\boldsymbol{C}_g + \boldsymbol{U})A$ the wave-action flux. The wave energy $E = \frac{1}{2}\rho g a^2$, where a is the wave amplitude. The linear set of equations (2.2), (2.3), (5.1) and (5.2) then have a single set of characteristic or ray directions given by

$$\partial \boldsymbol{x}/\partial t = -G_k/G_\omega = \omega_k,$$

where ω_k is the group velocity of the linear waves.

For this steady problem, and by the radial symmetry, (5.1) becomes

$$(1/r)(\partial/\partial r)(r\boldsymbol{B}\cdot\boldsymbol{e}_r) = 0. \tag{5.3}$$

For our choice of axisymmetric current (2.4), and for $B = |\boldsymbol{B}|$, (5.3) integrates to

$$RB\cos\alpha = RG_{k_r} a^2 = \text{constant}. \tag{5.4}$$

For the linear waves considered here, the wave-action flux $B = E/2k$. Thus (5.4), on substitution from (2.17) and (2.18), becomes

$$R^2 \sin 2\alpha E = \text{constant}. \tag{5.5}$$

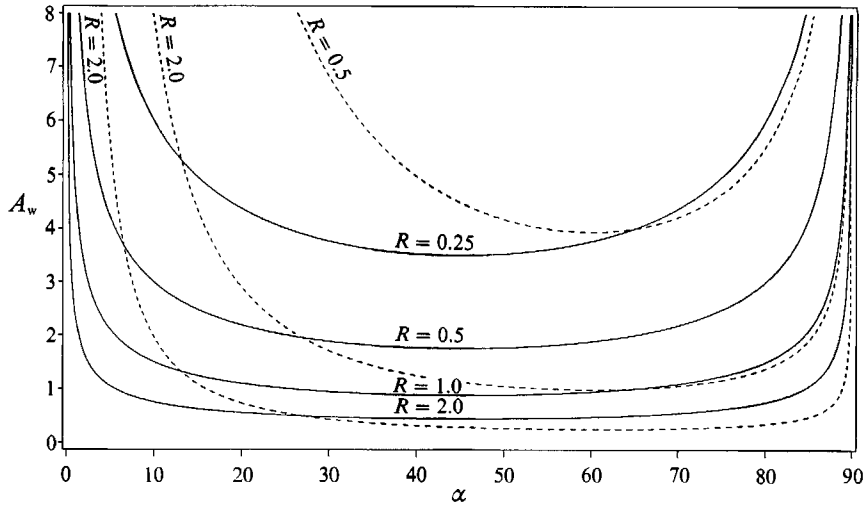

FIGURE 15. The variation of the linear wave amplitude A_w (——) and steepness KA_w (– – – –) as a function of the response angle α for various R-values. The initial angle $\phi_0 = 65°$ (concave currents) or $\phi_0 = 115°$ (convex currents).

With the assumption that on the boundary, where $R \to 1$, $V = 0$ and $\theta_0 = 0$, so that $\alpha_0 \equiv (\phi - \theta)_0 = \phi_0$ and $E = E_0$, (5.5) gives

$$A_w = a/a_0 = (E/E_0)^{\frac{1}{2}} = R^{-1}[\sin 2\phi_0/\sin 2\alpha]^{\frac{1}{2}} \tag{5.6}$$

$$= \frac{(R^{-1}\cos\phi_0)^{\frac{1}{2}}[R\ \mathrm{cosec}\ \phi_0 - V]^2}{R\ \mathrm{cosec}\ \phi_0\{[R\ \mathrm{cosec}\ \phi_0 - V]^4 - (R\ \mathrm{cosec}\ \phi_0)^2\}^{\frac{1}{4}}}. \tag{5.7}$$

It is important to note the difference between the theory presented above and the alternate configuration of waves originating at a point r_0, where $V = V_0$, which may or may not be zero, and where the initial angle $\sin\alpha = \sin\alpha_0$. For the latter configurations (2.6) gives

$$\begin{aligned} m &= r_0 k_0 \sin\alpha_0 \quad \text{at a radius} \quad r = r_0, \quad \text{where} \quad V = V_0; \\ &= r_1 k_0 \sin\alpha_1 \quad \text{at a radius} \quad r = r_1, \quad \text{where} \quad V = V_0; \\ &= r_2 k_2 \sin\alpha_2 \quad \text{at a radius} \quad r = r_2, \quad \text{where} \quad V = V_2. \end{aligned}$$

Thus, for (say) $V_0 = 0$, but at $r = r_1$, $\sin\alpha_1 = (r_0/r_1)\sin\alpha_0 = R^{-1}\sin\alpha_0$, so that

$$\cos\alpha_1 = (1 - R^{-1}\sin^2\alpha_0)^{\frac{1}{2}}.$$

Equation (5.7), for $V_0 = 0$ and with ϕ_0 replaced by $(\phi - \theta)_0 = \alpha_0$, then gives

$$A_w = a/a_0 = R^{-\frac{1}{2}}[\cos\alpha_0/\cos\alpha_1]^2,$$

which is in agreement with Peregrine (1981).

The ratio (5.6), as well as the linear steepness KA_w, is shown graphically in figure 15 as a function of the angle α for various values of R and for the initial angle $\phi_0 = 65°$ (for concave currents) or $\phi_0 = 115°$ (for convex currents). Comparison of figure 15 with figure 8 of Peregrine (1976) shows that the linear amplification of waves on a curved current proceed in a similar fashion to those on a parallel shear flow, except that larger and steeper waves can be expected on convex currents ($R < 1$) than on straight or concave currents ($R > 1$).

6. Validity of solutions

In all ray calculations it is assumed a plane-wave solution will apply and thus that all length and time scales present are much greater than the wavelength and period of the waves. If, in addition, the wave amplitude, a, is also assumed to be slowly varying, the expression (5.1) for the conservation of wave action is obtained.

It is clear from (5.4) that the linear wave amplitude, a, will become singular when $R \to 0$ or when $G_{k_r} \to 0$. The first case, when $R \to 0$, was shown to correspond to the so-called short-wave singularity. This is when the waves are refracted so much that their wavelength becomes very short and the small-amplitude approximation is no longer valid since the waves become too steep. In practice the waves probably break and dissipate.

It can be seen from (5.5), and is also shown in figure 15, that $G_{k_r} \to 0$ when $\alpha \to 0°$ or when $\alpha \to 90°$. On both following and opposing currents wave reflections imply $\alpha = 90°$ and $G_{k_r} = 0$. The rays are tangent to a caustic curve and ray theory thus fails in the neighbourhood of the caustic. The second case shown in figure 15, when $\alpha \to 0$, corresponds to the limit $V \to -\infty$, or $R \to 0$. The first limit is not realistic in practical applications, while the limit $R \to 0$ was shown to correspond to the so-called short-wave singularity. In the limit $R = 0$ the rays will be radially oriented and with a focus of rays at the origin. The plane-wave approximation will thus also not apply at the origin.

In situations where the waves are blocked by the current $G_{k_\theta} \to 0$ so that the ray solution will remain valid. For stopped waves, (3.4) and (3.6) apply. Ray theory will remain valid for all α-values except when $\alpha = 90°$ and the stopping and reflection conditions occur simultaneously. However, at stopping the waves may become sufficiently steep for nonlinear effects to become important and they may also break. At stopping the small-amplitude approximation may thus become invalid.

7. Caustic solutions

In §6 we indicated the singular behaviour of the slowly varying-wave approximation at a caustic. The linear theory itself, however, is not singular and there are available uniformly valid small-amplitude wave approximations which include caustics. McKee (1974), Peregrine (1976) and Peregrine & Smith (1975, 1979) gives examples for straight caustics in an inhomogeneous medium. For a curved caustic in an inhomogeneous medium the analysis is similar to that of Peregrine & Smith (1979).

Consider a family of rays which are refracted by the annular current (2.4) to form a curved caustic. The linear dispersion relation for axisymmetric sinusoidal waves in a frame of reference moving radially across the annulus with group velocity c_g is then

$$\omega = \sigma(k_r, k_\theta, r) + k_\theta U_\theta(r) - c_g k_r. \tag{7.1}$$

Here, as before, the r-dependence of (7.1) is considered to vary on a larger scale than that of ω and $\boldsymbol{k}$. If the radius of the caustic curve is denoted by $r = r_0$, and the local wave parameters there are ω_0 and $\boldsymbol{k}_0$, (7.1) becomes

$$\omega_0 = \sigma(k_{r_0}, k_{\theta_0}, r_0) + \kappa_{\theta_0} U_\theta|_0 - c_{g_0} k_{r_0}$$

so that in the neighbourhood of the caustic:

$$0 = \left.\frac{\partial \sigma}{\partial k_r}\right|_0 - c_{g_0}, \qquad 0 = \left.\frac{\partial \sigma}{\partial k_\theta}\right|_0 + U_\theta|_0.$$

Expanding about $\boldsymbol{k}_0$ and r_0, and if the leading-order contributions in wavenumber and position are retained, (7.1) becomes the perturbation dispersion relation

$$\hat{\omega} = (r-r_0)\frac{\partial\sigma}{\partial r}\bigg|_0 + \left(k_\theta \frac{\mathrm{d}U_\theta}{\mathrm{d}r}\right)\bigg|_0 + \tfrac{1}{2}\hat{k}_r^2 \frac{\partial^2\sigma}{\partial k_r^2}\bigg|_0, \tag{7.2}$$

where the perturbation frequency $\hat{\omega} = \omega - \omega_0$ and the perturbation wavenumber $\hat{\boldsymbol{k}} = \boldsymbol{k} - \boldsymbol{k}_0$.

If the wave amplitude is also considered to vary slowly, then the small frequency and wavenumber perturbations may be associated with space and time derivatives of the complex amplitude a. That is, if we identify

$$\hat{\omega} \quad \text{with} \quad \mathrm{i}\frac{\partial}{\partial t}, \qquad \hat{k}_r \quad \text{with} \quad -\mathrm{i}\frac{\partial}{\partial r},$$

the steady form of (7.2) reduces to

$$-2(r-r_0)\left[\frac{\partial\sigma}{\partial r}\bigg|_0 + \left(k_\theta \frac{\mathrm{d}U_\theta}{\mathrm{d}r}\right)\bigg|_0\right]a + \frac{\partial^2\sigma}{\partial k_r^2}\bigg|_0 \frac{\mathrm{d}^2 a}{\mathrm{d}r^2} = 0. \tag{7.3}$$

The appropriate solution of the Airy equation (7.3) is

$$a = a_0 \,\mathrm{Ai}\,(\eta), \tag{7.4}$$

with

$$\eta = \rho\left[\frac{2(\partial\sigma/\partial r|_0 + k_{\theta_0}\,\mathrm{d}U_\theta/\mathrm{d}r|_0)}{\partial^2\sigma/\partial k_r^2|_0}\right]^{\frac{1}{3}},$$

$$\rho = r - r_0.$$

The complex constant a_0 is found by matching the asymptotic formula of the Airy function

$$\mathrm{Ai}(\eta) \sim -\frac{\sin\left[\frac{2}{3}(-\eta)^{\frac{3}{2}} + \frac{1}{4}\pi\right]}{\pi^{\frac{1}{2}}(-\eta)^{\frac{1}{4}}},$$

for large negative values of η, with the ray solution.

When the results of this section are compared with §6 of Peregrine & Smith (1979), it is clear that, for our axisymmetrical representation, the caustic results are similar to those obtained for a straight caustic in an inhomogeneous medium. A uniformly valid Airy function representation, similar to that given by (6.9)–(6.11) of that paper, will thus also apply here.

8. Conclusions

Exact linear solutions for the interaction of steady axisymmetric deep-water gravity waves and an axisymmetric annular current have been derived. Two important non-dimensional parameters, namely a current velocity parameter, $V = U_\theta/c_0$, and a radius-angle parameter, R cosec ϕ_0, where $R = r/r_0$, were identified. $R > 1$ corresponds to concave currents while convex currents have $R < 1$.

For linear waves the radius at which the waves will be reflected, blocked and stopped by the current was calculated. For this current configuration the waves will nearly always be blocked before they are stopped, the exception being when the blocking and stopping contours cross and both conditions occur simultaneously. At both blocking and stopping the ray solutions will remain valid, while at stopping the small-amplitude wave approximation may no longer hold.

Both positive convex currents and positive concave currents admit reflections, but reflections are only possible for negative convex currents. Reflections may also occur on opposing convex currents before the waves are blocked. On negative concave currents the linear waves may also be stopped by the current, but very large opposing current velocities are required. Furthermore, reflections on an adverse convex current will occur more frequently than the stopping velocity criterion can be satisfied. This is so since large negative values of V are needed to stop the waves. One exception is when, at the point of reflection, a stopping velocity caustic is formed when $V = -\frac{1}{4}$. The linear radius at this point is $R = \frac{1}{4}\sin\phi_0$.

Wave rays may also be trapped within the boundaries of the current. Waves that are generated on still water inside the annulus, and which penetrate the annulus, while travelling in the same direction as the concave current, may undergo multiple reflections and remain trapped within a certain reflection radius of the current. Only waves generated within the boundaries of the annulus can be trapped so as to remain within the annulus. For a positive convex current configuration an example was presented in §4. The theory presented in this paper limits the waves, and therefore also the current distributions, to cases where $R\,\mathrm{cosec}\,\phi_0 > 1$. Figure 7 then shows that it is not possible to construct an adverse current configuration which can trap waves.

In all of the above examples it was assumed that the singularities occur within the boundaries of the describing current annulus. In a real life application it may be found that the waves penetrate or leave the annulus before the caustic is reached. Furthermore, since only steady, axisymmetrical waves were considered in this study, focusing effects associated with waves incident from a preferred direction could not be studied. It is, however, important to note that for other wave fields the *individual* rays will be as calculated in this study, but that the overall picture for a steady wave field will be made up of a family of such rays which may be very different from the axisymmetrical wave field considered here. For example, figure 16 shows one example of such unidirectional rays incident upon an annular current with velocity profile as shown. The resulting cusps and caustics are clearly defined and do not, as for axisymmetric waves, occur at fixed radii.

The axisymmetrical representation considered here also restricts, for both concave and convex currents the practical application of the theory to two distinctly different types of wave fields. For concave currents the wave field inside the annulus is assumed to be spreading outward from, for example, a localized storm or a point source. In contrast convex currents have waves approaching the annulus from the outside and are therefore constrained to be converging inwards. This is a more uncommon physical situation and may, for example, be due to a rapidly travelling storm system if the propagation speed of the front is greater than the group velocity of the generated waves.

An inwardly converging wave field can also result when a uniform wave field encounters a ring-like current structure and the waves are focused into a cusp by the current. All the major Western boundary currents of the world regularly shed eddies, plumes or rings which may then lead to focusing of the rays onto the original current. For the particular case of the Agulhas Current on the south-east coast of South Africa, Lutjeharms, Catzel & Valentine (1989) calculated that one shear edge feature, such as described above, is present 65% of the time. Two or more features occur 36% of the time. Gründlingh (1988, and private communication 1990) has also established that cold-core cyclonic rings commonly occur off the Agulhas Current. The surface current velocities associated with these rings can exceed 1 m/s while their predicted

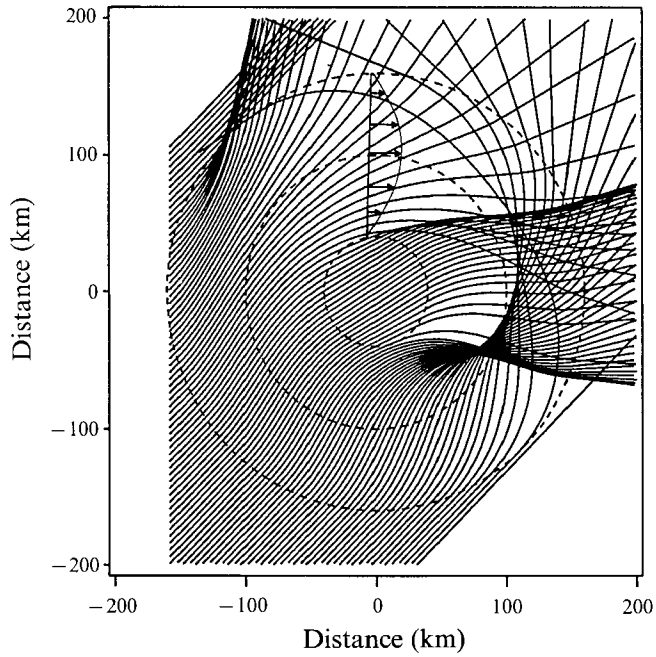

FIGURE 16. Numerical simulation of unidirectional rays incident upon an annular current. The outer radius of the current was taken as 160 km while the inner radius was 40 km. The period of the incident waves $T = 10$ s while the maximum current velocity $U_\theta = 2.0$ m/s. An incidence angle of 45° was used for the rays.

lifetimes are in excess of 18 months. For the particular case of the Agulhas current, the influence of certain current parameters on the resulting focusing of the waves was examined by Gerber (1991).

For the particular application of waves interacting with the Agulhas Current (north of 34° S) on the east coast of South Africa, a convex current situation will apply. With an approximate radius $r_0 = 1400$ km and for an average width of the current of 140 km, only $R = r/r_0$ values in the range $0.9 < R < 1.0$ will apply.

The author is pleased to acknowledge useful discussions with Professor D. H. Peregrine.

REFERENCES

BRETHERTON, F. P. & GARRETT, C. J. R. 1968 Wavetrains in inhomogeneous moving media. *Proc. R. Soc. Lond.* A**302**, 529–554.

GERBER, M. 1991 Giant waves and the Agulhas Current. *Deep-Sea Res.* (submitted).

GRÜNDLINGH, M. L. 1988 Review of cyclonic eddies of the Mocambique ridge current. *S. Afr. J. Mar. Sci.* **6**, 193–206.

HOLTHUIJSEN, L. H. & TOLMAN, H. L. 1991 Effects of the Gulf Stream on ocean waves. *J. Geophys. Res.* **96**, 12755–12771.

LONGUET-HIGGINS, M. S. & STEWART, R. W. 1960 Changes in the form of short gravity waves on long waves and tidal currents. *J. Fluid Mech.* **8**, 565–583.

LONGUET-HIGGINS, M. S. & STEWART, R. W. 1961 The changes in amplitude of short gravity waves on steady non-uniform currents. *J. Fluid Mech.* **10**, 529–549.

LUTJEHARMS, J. R., E., CATZEL, R. & VALENTINE, H. R. 1989 Eddies and other boundary phenomena of the Agulhas Current. *Continental Shelf Res.* **9**, 597–616.

MALLORY, J. K. 1974 Abnormal waves on the south east coast of South Africa. *Intl Hydrog. Rev.* **51**, 99–129.

MCKEE, W. D. 1974 Waves on a shearing current: a uniformly valid asymptotic solution. *Proc. Camb. Phil. Soc.* **75**, 295–301.

MEYER, R. E. 1979 Theory of water-wave refraction. *Adv. Appl. Mech.* **19**, 53–141.

PEREGRINE, D. H. 1976 Interactions of water waves and currents. *Adv. Appl. Mech.* **16**, 9–117.

PEREGRINE, D. H. 1981 Refraction of finite-amplitude water waves: deep-water waves approaching circular caustics. *J. Fluid Mech.* **109**, 63–74.

PEREGRINE, D. H. & SMITH, R. 1975 Stationary gravity waves on non-uniform free streams: jet-like flows. *Math. Proc. Camb. Phil. Soc.* **77**, 415–438.

PEREGRINE, D. H. & SMITH, R. 1979 Nonlinear effects upon waves near caustics. *Phil. Trans. R. Soc. Lond.* A**292**, 341–370.

PHILLIPS, O. M. 1978 *The Dynamics of the Upper Ocean.* Cambridge University Press.

SAVITSKY, D. 1970 Interaction between gravity waves and finite turbulent flow fields. In *8th Symp. on Naval Hydrodynamics*, pp. 389–446. Office of Naval Res. Arlington, Va.

SMITH, R. 1976 Giant waves. *J. Fluid Mech.* **77**, 417–431.

WHITHAM, G. B. 1962 Mass, momentum and energy flux in water waves. *J. Fluid Mech.* **12**, 135–147.